Cellular/Molecular

# Interplay among cGMP, cAMP, and $Ca^{2+}$ in Living Olfactory Sensory Neurons *In Vitro* and *In Vivo*

**Mara Pietrobon,[1]* Ilaria Zamparo,[1]* Micol Maritan,[1] Sira Angela Franchi,[1] Tullio Pozzan,[1,2,3] and Claudia Lodovichi[1,3]**

[1]Venetian Institute of Molecular Medicine, 35129 Padova, Italy, [2]Department of Biomedical Sciences, University of Padova, 35121 Padova, Italy, and [3]Consiglio Nazionale della Ricerche, 00185 Rome, Italy

**The mechanism of cGMP production in olfactory sensory neurons (OSNs) is poorly understood, although this messenger takes part in several key processes such as adaptation, neuronal development, and long-term cellular responses to odorant stimulation. Many aspects of the regulation of cGMP in OSNs are still unknown or highly controversial, such as its subcellular heterogeneity, mechanism of coupling to odorant receptors and downstream targets. Here, we have investigated the dynamics and the intracellular distribution of cGMP in living rat OSNs in culture transfected with a genetically encoded sensor for cGMP. We demonstrate that OSNs treated with pharmacological stimuli able to activate membrane or soluble guanylyl cyclase (sGC) presented an increase in cGMP in the entire neuron, from cilia-dendrite to the axon terminus-growth cone. Upon odorant stimulation, a rise in cGMP was again found in the entire neuron, including the axon terminus, where it is locally synthesized. The odorant-dependent rise in cGMP is due to sGC activation by nitric oxide (NO) and requires an increase of cAMP. The link between cAMP and NO synthase appears to be the rise in cytosolic $Ca^{2+}$ concentration elicited by either plasma membrane $Ca^{2+}$ channel activation or $Ca^{2+}$ mobilization from stores via the guanine nucleotide exchange factor Epac. Finally, we show that a cGMP rise can elicit both *in vitro* and *in vivo* the phosphorylation of nuclear CREB, suggesting that this signaling pathway may be relevant for both local events (pathfinding, neurotransmitter release) and more distal processes involving gene expression regulation.**

## Introduction

Upon activation of the odorant receptor (OR) expressed at the cilia (Menini, 1999) and the axon terminus (Maritan et al., 2009), a rise of cAMP and $Ca^{2+}$ is locally generated. Several studies have demonstrated that odor exposure promotes the synthesis of another second cyclic messenger, cGMP. Compared with the odor-induced rise of cAMP, cGMP presented a slow and sustained rise. This dynamic suggested that cGMP may not be involved in initial stimulus detection events, but rather may be involved in several important long-term cellular responses to odor stimulation (Kroner et al., 1996; Zufall and Leinders-Zufall, 1998).

cGMP is produced by two different enzymes: membrane guanylyl cyclase (mGC) and soluble GC (sGC), both present in olfactory sensory neurons (OSNs) (Lucas et al., 2000). Although the function and the ligands of mGC in OSNs are largely unknown, at least two types of mGCs have been described in OSNs: the cilia mGC expressed in most adult OSNs (Moon et al., 1998), and the mGC-D, expressed by a subset of OSNs that present a unique signaling transduction pathway (Juilfs et al., 1997; Leinders-Zufall et al., 2007).

Soluble GCs are heterodimers that are activated by gaseous messengers: nitric oxide (NO) and carbon monoxide (CO). NO is produced by nitric oxide synthase (NOS) (Dellacorte et al., 1995), transiently expressed in OSNs during development and in regenerating neurons (Roskams et al., 1994; Chen et al., 2003, 2004), while CO is synthesized by the enzyme heme oxygenase (HO), mostly expressed in adult OSNs (Verma et al., 1993; Boehning et al., 2003). Many aspects of cGMP generation and signaling remain poorly understood, and the available data are often contradictory. In particular, whether cGMP is produced only at the cilia or also in other OSN compartments, the mechanism of OR coupling to GCs and the downstream target of cGMP remain unanswered questions. A major obstacle at addressing such questions has been the use, thus far, only of approaches with modest spatial and temporal resolution, which allow cGMP average measurement on cell population (radioimmunoassay). Our data, performed for the first time in single living OSNs in culture, demonstrate that upon pharmacological and physiological (odors) stimuli a rise in cGMP is triggered in the entire neuron from cilia-dendrite to the axon terminus, where it is locally synthesized upon local OR activation.

We found that odor-induced cGMP synthesis is due to sGC activation via NO and requires an increase in cAMP. The link between cAMP and sGC activation appears to be a rise of $Ca^{2+}$, due to plasma membrane $Ca^{2+}$ channel activation and $Ca^{2+}$ mobilization from stores. In the latter case, the link between cAMP rise and $Ca^{2+}$ mobilization is not the canonical target of

Received Dec. 23, 2010; revised April 7, 2011; accepted April 15, 2011.

Author contributions: C.L. designed research; M.P., I.Z., M.M., and S.A.F. performed research; M.P., I.Z., M.M., S.A.F., and C.L. analyzed data; T.P. and C.L. wrote the paper.

This research was supported by the Armenise Harvard Career Development Award (C.L.), Cariparo Foundation and Italian Ministry of the University (T.P.), IIT Grantto (T.P.), and the Strategic Project, University of Padua (T.P.). We are grateful to Wolfgang Dostmann for generously providing the cGMP sensor, Cygnet 2.1. We thank Paolo Lorenzon for helping with experiments and all members of our laboratory for valuable comments.

*M.P. and I.Z. contributed equally to this work.

Correspondence should be addressed to Claudia Lodovichi, Venetian Institute of Molecular Medicine (VIMM), Via Orus 2, 35129 Padova, Italy. E-mail: claudia.lodovichi@unipd.it or lodovichi.c@gmail.com.

M. Maritan's present address: Institut Cochin, Université Paris Descartes, Department of Endocrinology, Metabolism, and Cancer CNRS (UMR 8104), Paris, France.

DOI:10.1523/JNEUROSCI.6722-10.2011

 0270-6474/11/318395-11$15.00/0

cAMP, protein kinase A (PKA), but rather the guanine nucleotide exchange factor Epac. Furthermore, we show that treatment of OSNs *in vitro*, and of the axon termini of the OSNs on the bulb *in vivo*, with odors or 8Br-cGMP, a membrane-permeable analog of cGMP, is associated to CREB phosphorylation at the nuclear level.

## Materials and Methods

*Primary culture of olfactory sensory neurons*

The olfactory epithelium was harvested from embryonic rats (E18–19) in ice-cold HBSS (Invitrogen). Tissue was enzymatically dissociated in 5 ml of 0.125% trypsin at 37°C in a water bath for 15 min. The enzymatic digestion was stopped by adding 1 ml of fetal bovine serum (FBS). The dissociated cells were then washed for 3 min three times with 5 ml of prewarmed HBSS. The cells were pelleted by centrifugation (800 × *g* for 4 min), and the cell pellet was resuspended in 5 ml of prewarmed culture medium by gentle pipetting and plated onto 24 mm glass coverslips coated with poly-L-lysine (Sigma). The cells were maintained in culture medium (D-Val Mem, 10% FBS, 5% Nu Serum, Penstrep L-glutamine, 100U/ml (Invitrogen), 10 μM Ara C (Sigma), and 25 ng/ml NGF (BD Biosciences) under standard conditions (Ronnett et al., 1991, Liu et al., 1998). After 6–24 h in culture, cells were transiently transfected with the protien kinase G (PKG)-based sensor for cGMP (Cygnet 2.1) (Honda et al., 2001) or with the genetically encoded $Ca^{2+}$ sensor, targeted to the endoplasmic reticulum lumen, D1ER (Rudolf et al., 2006), with Transfectin (Bio-Rad) transfection reagent, or loaded with 5 μM fura 2-AM (Invitrogen) at 37°C for 30–40 min.

All cells used in this study were clearly identifiable as OSNs by their characteristic bipolar morphology, having a single thick dendrite with knob-like swelling and cilia emanating from it, and a thin long axon. OSNs in culture expressed the specific marker olfactory marker protein (OMP) (see Fig. 1*A*), a marker expressed by mature, functioning OSNs.

After transfection, cells were maintained in culture for an additional 12–15 h before FRET imaging experiments to allow the genetically encoded sensors to be expressed. In transfected cells, the fluorescence is evenly distributed throughout the cytoplasm and is excluded from the nucleus. The morphology of OSNs transfected with Cygnet 2.1 or with D1ER appear normal and undistinguishable from nontransfected cells.

*cGMP measurements in cultured neurons*

FRET imaging experiments were performed on an inverted microscope Olympus IX 70 with a 60× NA 1.4 oil-immersion objective. The microscope was equipped with an illumination system and CCD camera TILLvisION v3.3 equipped with the polychrome IV. Excitation was 430 nm. Emission wavelengths were separated with a dual-emission beam splitter (Multispec Microimager; Optical Insights) with a 505 nm dichroic filter and 480 ± 15 and 545 ± 20 nm emission filters for CFP and YFP, respectively. All filters and dichroics were from Chroma Technology. Live images were acquired for 200–300 ms at 5 s intervals.

The day of the experiment, coverslips were mounted in an imaging chamber at room temperature (RT) and maintained in Ringer's solution as follows (in mM): 140 NaCl, 5 KCl, 1 $CaCl_2$ $2H_2O$, 1 $MgCl_2$, 10 HEPES, 10 glucose, 1 sodium pyruvate, pH 7.2. Images were acquired using TILLvisION v3.3 software and then processed off-line using a custom-made software (Vimmaging made in Mat Lab environment). FRET changes were measured as changes in the background-subtracted 480/545 nm fluorescence emission intensities on excitation at 430 nm and expressed as $R/R_0$, where $R$ is the ratio at time $t$ and $R_0$ is the ratio at time = 0 s. The time for half-maximal response ($t_{1/2}$), was evaluated as the time, after stimulus application, at which half-maximal response was reached, considering half-maximal response = $(R - R_0)/2 + R_0$, and $t = t - t_0$, where $t_0$ is stimulus application time and $t$ is time at the peak of the response.

The changes in CFP/YFP ratios reported in all the experiments were always dependent on an antiparallel behavior of CFP and YFP fluorescence.

At longer times, during the experiments the two wavelengths might decrease in parallel, probably due to an out of focus artifact and/or bleaching. The CFP/YFP ratio, however, compensates for this artifact, and the ratio trace remains practically constant. The ability of the ratio measurements to compensate for parallel changes in the two wavelengths is a well known advantage of this approach.

*$Ca^{2+}$ measurements in cultured neurons*

$Ca^{2+}$ imaging experiments were performed on an inverted Olympus IX 70 microscope with a 40× NA 1.3 oil-immersion objective (see above for details). Changes in intracellular $Ca^{2+}$ were visualized using 380/15 nm and 340/15 nm excitation filters and 510/40 nm emission filter, and were acquired for 100–200 ms every 5 s. Images were then processed off-line using ImageJ software (National Institutes of Health). Changes in fluorescence (340/380 nm) was expressed as $R/R_0$, where $R$ is the ratio at time $t$ and $R_0$ is the ratio at time = 0 s.

*cGMP and $Ca^{2+}$ measurements in the same cultured neurons*

After 6–24 h in culture, cells were transfected with the PKG-based sensor for cGMP, as above. The day of the imaging experiments, neurons transfected with the PKG-based sensor were loaded with fura-2. FRET experiments were conducted according to the standard protocol (see above). Changes in intracellular $Ca^{2+}$ were visualized using a 380/15 nm excitation filter and 480 ± 15 and 545 ± 20 nm emission filters. Live images were acquired for 200–300 ms every 6 s. Images were then processed off-line using ImageJ (National Institute of Health). To measure FRET ratios, bleed through of CFP and fura-2 was corrected. To analyze fura-2 fluorescence intensity, fura-2 emission from both channels was summed, and bleed through from CFP was corrected (Dunn et al., 2009).

*$Ca^{2+}$ measurements with a genetically encoded $Ca^{2+}$ sensor, targeted to the endoplasmic reticulum (D1ER) in primary culture of OSN*

FRET imaging experiments were performed on an inverted Olympus IX 70 microscope with a 60× NA 1.4 oil-immersion objective (see above for details). In this case, FRET changes were measured as changes in the background-subtracted 545/480 nm fluorescence emission intensities on excitation at 430 nm. Live images were acquired for 200–300 ms at 5 s intervals.

*Stimuli on OSN* in vitro

Pharmacological stimuli: atrial natriuretic peptide (ANP, 1 μM), activator of mGCs; *S*-nitroso-*N*-acetylpenicillamine (SNAP; 300 μM), an NO donor that activates sGCs; forskolin (Frsk; 25 μM), generic activator of adenylyl cyclase (AC); 8 Br-cGMP (50 μM), a membrane-permeable cGMP analog; 1-methyl-3-isobutylxanthine (IBMX; 250 μM), nonselective inhibitor of phosphodiesterases (PDEs); zaprinast (250 μM, Alexis), inhibitor of the cGMP-specific PDE-5; SQ22536 (30 μM; Biomol International), inhibitor of AC; LY83583 (10 μM; Calbiochem), inhibitor of sGC; zinc protoporphyrin IX (ZnPP9) (10 μM Calbiochem), inhibitor of HO that produces CO; 7 nitroindazole (7-NI) (30 μM; Calbiochem), inhibitor of NOS that produces NO; H89 (10 μM; Biomol International), inhibitor of PKA; KT5720 (1 μM, Calbiochem) inhibitor of PKA; Ringer's solution with high concentration of KCl (50 mM); 8-CPT-2′-O-Me-cAMP (30 μM) activator of Epac; U73122 (30 μM) inhibitor of phospholipase Cε (PLCε) all from Sigma, unless stated otherwise, were prepared in stocks and diluted to the final concentration (indicated in brackets) in the bath.

The odorant stimuli were represented by mixtures of several compounds, including the following: citralva, citronellal, menthone, carvone, eugenol, geraniol, acethophenone, hexanal, benzyl alcohol, heptanoic acid, propionic acid, benzaldehyde, and IBMP (all from Sigma) prepared as 1 mM stock in Ringer's solution and diluted to the final concentration of 1, 50, or 200 μM for each odorant in the bath. These odor concentrations are well within the range (1 nM–1 mM) of those used in previous studies (Bozza and Kauer, 1998; Bhandawat et al., 2005, 2010) on dissociated OSNs. The stimuli baths applied were carefully and slowly delivered via an application pipette positioned far away (~3 mm) from the cell to obtain a homogeneous distribution of the stimulus in the bath, capable of stimulating the entire cells and not a specific compartment.

Odor stimuli were also focally applied to the growth cone of OSNs in culture (with no perfusion) by a single-puff pressure ejection (Pneumatic

pico-pump, WPI) with a glass micropipette (3–5 $\mu$m tip diameter, 3 s puff duration, 5 psi). The micropipette was positioned at 5–10 $\mu$m from the growth cone. Concentration of odors in the micropipette was 1 mM for each component of the mixture. The volume ejected from the pipette was very small (5–10 nl) and got diluted in the Ringer's solution of the chamber (1 ml). Thus, the concentration of the stimulus focally applied at the axon terminus-growth cone was much lower than the concentration of the stimulus present in the pipette, but sufficient to induce OR activation. The stimulus gets even more diluted as it spreads away from the site of application. Thus, the spreading of the stimulus to the rest of the cell did not represent a risk of triggering the cGMP rise in other compartments. To focally applied stimuli at the axon termini, we modified the protocol used by Lohof et al. (1992).

The neurons were continuously perfused with normal Ringer's solution (1.5 ml/min) except during stimulus presentation. Stimuli were bath applied for 4–10 s, in $Ca^{2+}$ imaging experiments, and for 5–7 min in FRET imaging experiments, or for the entire duration of the experiments.

Stimuli applied *in vivo*, on the olfactory bulb (OB), had the following concentrations: 8Br-cGMP, 250 $\mu$M; odors, 1 mM; Ly 83583, 250 $\mu$M.

### *Immunostaining*

*OMP.* Cells in culture were fixed in ice-cold methanol 100% for 20 min at RT. Cells were then reacted with goat polyclonal antibodies specific for OMP (Wako Chemicals) at 1:1000 dilution. The bound primary antibody was visualized using Cy3-conjugated anti-goat IgG (Jackson Laboratories).

*Epac, sarcoendoplasmic reticulum $Ca^{2+}$ ATPase, calreticulin.* After 48 h in culture, cells were fixed with 4% paraformaldehyde in 0.1% phosphate buffer. Cell were then reacted with rabbit polyclonal antibody specific for EPAC1 (1:100, Abcam), or mouse polyclonal antibody specific for sarcoendoplasmic reticulum $Ca^{2+}$ ATPase (SERCA) (1:100; Sigma) or rabbit polyclonal antibody specific for calreticulin (1:100; Abcam). The bound primary antibody was visualized using FITC-conjugated anti-goat IgG (1:500; Sigma), Cy3-conjugated anti-mouse IgG, and DyLight 488-conjugated anti rabbit IgG (1:500; Jackson Laboratories) respectively.

*Phosphorylated CREB* in vitro. Primary cultures of OSNs were treated with 8Br-cGMP (50 $\mu$M) and left in standard culture condition for 20–30 min. Cell were then fixed with 4% paraformaldehyde in 0.1% phosphate buffer for 20 min at RT. Cells were then reacted with rabbit polyclonal antibody specific for phosphorylated (P)-CREB (1:2000; Millipore). The bound primary antibody was then visualized using the ABC kit (Vectastain; Vector Laboratories).

*Phosphorylated CREB* in vivo. 18 mice (P15-P30) were anesthetized with Zoletil 100 (a combination of zolazepam and tiletamine, 1:1, 10 mg/kg; Laboratoire Virbac) and Xilor (xilazine 2%, 0.06 ml/kg; Bio98) and placed in a stereotaxic apparatus. The scalp was resected, and a small portion of the bone over the two bulbs removed. 8Br-cGMP (250 $\mu$M, $n = 4$), odor mixture (1 mM, $n = 4$), or odor mixture (1 mM) in the presence of the sGC inhibitor LY83583 (250 $\mu$M, $n = 5$) or Ringer's solution for controls ($n = 5$) were locally applied on the bulb with a pipette. To avoid possible effects due to diffusion of odors applied on the olfactory bulb, the experiments were performed under a chemical hood, and the nose of the animal was placed in a funnel connected to the vacuum for the entire duration of the experiments. After 30–40 min, animals were killed and transcardially perfused with 0.9% saline followed by 4% paraformaldehyde in 0.1% phosphate buffer. The epithelium was removed, postfixed overnight in a 4% paraformaldehyde, 0.1% phosphate buffer and then cryoprotected in 30% sucrose in PBS for 3 d. The epithelium was sectioned on the cryostat (20-$\mu$m-thick section). Epithelium sections were reacted with rabbit antibody specific for P-CREB (1:2000; Millipore). The bound primary antibody was visualized with the ABC kit (Vectastatin; Vector Laboratories).

*P-CREB analysis.* The signal intensity, background subtracted, of CREB phosphorylation in the nuclei of OSNs in culture and in olfactory epithelium coronal sections, was evaluated using ImageJ software. P-CREB levels were normalized to the P-CREB level present in controls. Student's *t* test, two tailed, not paired, was used to evaluate statistical significance.

All data are presented as mean ± SE. Student's *t* tests (two tailed, paired) was performed to evaluate statistical significance ($*p = 0.01 < p < 0.05$; $**p = 0.001 < p < 0.01$; $***p < 0.001$). The number of cells or animals analyzed is denoted by *n*.

## Results

### Physiological health status of isolated OSNs

Since in our study neurons remained in culture for a longer period of time (required to express the genetically encoded sensors) than in most studies on isolated olfactory neurons, we performed a series of control experiments to evaluate the healthy state of the OSNs in the time window in which FRET experiments were performed. (1) We carefully checked the morphology of the transfected cells. In particular, the transfected OSNs in culture for 2 d had the typical bipolar morphology (Figs. 1*A–D*, 2*A*) of OSNs and expressed specific markers of OSNs, such as OMP (Fig. 1*A*,*B*), as freshly plated OSNs; no signs of sufferance, such as membrane blebs, was observed in the vast majority (>90%) of the OSNs in culture for 2 d. (2) The cultured OSNs, both transfected and nontransfected, had similar functional responses and did not differ from freshly plated neurons.

Examples of the cytosolic $Ca^{2+}$ changes elicited by KCl depolarization or odors in cells kept in culture for 2 d are presented in Figure 1. The cells were loaded with the $Ca^{2+}$ indicator fura-2 and challenged with KCl (50 mM) and odors, at different concentrations (1, 50, and 200 $\mu$M). OSNs exhibited a fast onset, rapidly recovering $Ca^{2+}$ signal in response to KCl depolarization [total *n* ($n_{tot}$) = 13; responsive cells = 90%] (Fig. 1*E*), as observed in previous studies (Bozza and Kauer, 1998; Bozza et al., 2002). At all concentrations tested (1, 50, and 200 $\mu$M), well within the range (1 nM–1 mM) of those used in previous experiments on isolated OSNs (Bozza and Kauer, 1998; Bhandawat et al., 2005, 2010), odors elicited $Ca^{2+}$ responses (Fig. 1) indistinguishable from those obtained in freshly plated neurons.

As expected, due to the partial cross-reactivity of each OR for different odors (Malnic et al., 1999), the higher odor mix concentration used (200 $\mu$M) was able to elicit reliable responses in a higher number of cells (odor mix 1 $\mu$M, $n_{tot} = 29$, responsive cells = 6%; odor mix 50 $\mu$M, $n_{tot} = 30$, responsive cells = 16%; odor mix 200 $\mu$M, $n_{tot} = 39$, responsive cells = 33%).

Due to our experimental conditions (OSNs with unknown OR specificity and a single cell analyzed in each experiment), we then decided to use, in all the following experiments that required odor stimulation, the concentration of 200 $\mu$M, a condition that increases the probability of finding responsive cells.

Odor concentrations in the range of hundreds of micromolar have also been used in $Ca^{2+}$ imaging experiments performed on isolated OSNs expressing specific OR of known ligands (Touhara et al., 1999; Imai et al., 2006).

Noteworthy, when the odor mix was continuously present in the bath (at least 8 min) (Fig. 1*F*) the $Ca^{2+}$ signal did not return completely to baseline. When the odor mix was applied for 4–10 s and then washed away, the $Ca^{2+}$ signal returned to baseline (Fig. 1*G*). OSNs nonresponsive to odor mix were subsequently challenged with KCl (50 mM) to test their viability. A prompt rise in $Ca^{2+}$ was observed after KCl stimulation (Fig. 1*H*). These results indicate that the absence of response to odors is due to the specificity of the OR expressed by OSNs and exclude unspecific effects due to odor mixture application.

Together, these results demonstrate that OSNs in culture for 2 d (i.e., the time window in which FRET imaging experiments were carried out) are morphologically and functionally indistinguishable from freshly plated cells.

### cGMP dynamics in OSNs upon pharmacological stimulation

Primary cultures of OSNs were transiently transfected with the PKG-based sensor for cGMP, Cygnet (Honda et al., 2001) (Fig. 2*A*). Changes in cGMP levels result in modification of FRET between the YFP and CFP moieties genetically fused to PKG and can be conveniently monitored by the changes of the CFP/YFP fluorescence emission ratio (480/545 nm). A rise in CFP/YFP ratio reflects an increase in cGMP. It is noteworthy that Cygnet is a highly specific indicator of cGMP and is practically insensitive to cAMP levels (selectivity for cGMP over cAMP is >100:1) (Honda et al., 2001). A first series of experiments were performed using drugs that are known to activate mGCs and sGCs and/or to inhibit PDEs.

As shown in Figure 2*B*, ANP (1 $\mu$M), an agent known to activate mGCs in most, if not all, cell types, induced a rise in CFP/YFP ratio, as expected for an increase in cGMP. The increase in cGMP was observed in the entire OSN, from cilia-dendrite to axon terminus-growth cone. The rise of cGMP began with no appreciable lag phase between stimulus application and the onset of the cGMP rise, and remained sustained for the entire duration of the experiment (at least 8 min) (Fig. 2*B*). The time to reach half-maximal response ($t_{1/2}$) was faster at the cilia-dendrite and at the axon terminus-growth cone than at the soma level ($n = 6$, $t_{1/2}$: cilia-dendrite = 1.1 ± 0.2 min, soma = 1.5 ± 0.1 min, axon terminus-growth cone = 0.85 ± 0.2 min; *t* test $t_{1/2}$: cilia dendrite-soma, $^{*}p = 0.02$; axon terminus-growth cone-soma, $^{**}p = 0.005$; cilia dendrite-axon terminus-growth cone, $p = 0.19$).

When the OSNs were treated with NO donors, capable of activating the sGCs, such as SNAP (300 $\mu$M), a prompt rise in cGMP was observed again in the entire neuron, from cilia-dendrite to the axon terminus-growth cone (Fig. 2*C*). Also, in this case no latency was observed between stimulus application and the onset of the response. A variable lag time was observed if lower SNAP concentrations were used (data not shown). The time to reach half-maximal response was not statistically different in the compartments analyzed ($n = 6$, $t_{1/2}$: cilia-dendrite = 1.6 ± 0.3 min; soma = 1.8 ± 0.4 min; axon terminus-growth cone = 1.6 ± 0.3 min).

In a variety of cell types (including OSNs), cAMP is produced in resting cells in the absence of external stimuli, due to the constitutive activity of ACs. To determine whether this is the case also for cGMP, OSNs were treated with zaprinast (250 $\mu$M), an inhibitor of PDE5 (that specifically hydrolyzes cGMP) or IBMX (250 $\mu$M), a nonspecific PDE inhibitor (Lugnier, 2006). As shown in Figure 2*D*, no cGMP increase could be detected in OSNs upon application of zaprinast, although all cells responded to ANP applied subsequently ($n = 4$) with the same kinetics observed for ANP, used as first stimulus (Fig. 2*B*), faster at the cilia-dendrite and at the axon terminus-growth cone than at the soma (*t* test $t_{1/2}$ cilia dendrite-soma, $^{*}p = 0.02$; axon terminus-growth cone soma, $^{*}p = 0.04$; cilia dendrite-axon terminus-growth cone, $p = 0.4$). IBMX, instead, caused a substantial, slow rise in cGMP in the entire neuron (Fig. 2*E*) ($n = 4$, $t_{1/2}$: cilia-dendrite = 2.5 ± 0.4 min; soma = 3 ± 0.6 min; axon terminus-growth cone = 2.5 ± 0.5 min). It is noteworthy that the cGMP increases elicited by the above-mentioned drugs have been observed in the majority (>90%) of the neurons tested.

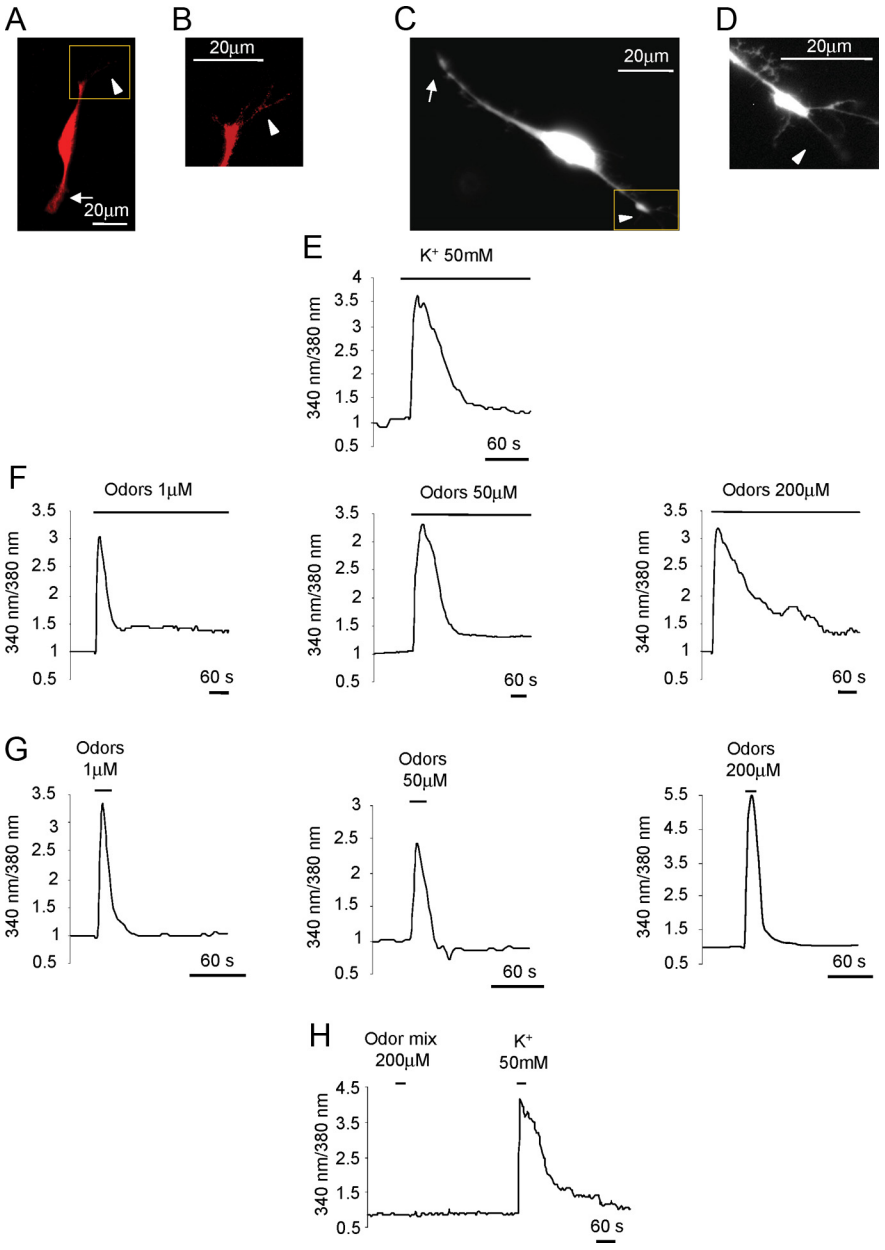


**Figure 1.** $Ca^{2+}$ dynamics in OSN in culture. ***A***, Example of an OSN immunopositive for OMP. ***B***, Higher magnification of the cilia indicated in the square in ***A***. ***C***, Example of an OSN loaded with fura-2. ***D***, Higher magnification of the cilia emanating from the knob, indicated in the square in ***C***. Arrows, Axon terminus-growth cone; arrowheads, cilia-dendrite. Scale bar, 20 $\mu$m. ***E–H***, Normalized fluorescence ratio changes (340/380 nm) in OSN loaded with fura-2 and challenged with KCl (50 mM), bath applied (***E***); odor mixture at 1, 50, 200 $\mu$M, bath applied (***F***); odor mixture at 1, 50, 200 $\mu$M, bath applied for 4–10 s (***G***); example of a nonresponsive neuron to the odor mixture (200 $\mu$M, bath applied for 4–10 s), but responsive to KCl (50 mM) bath applied for 4–10 s (***H***). Primary culture of OSNs were used in all experiments.

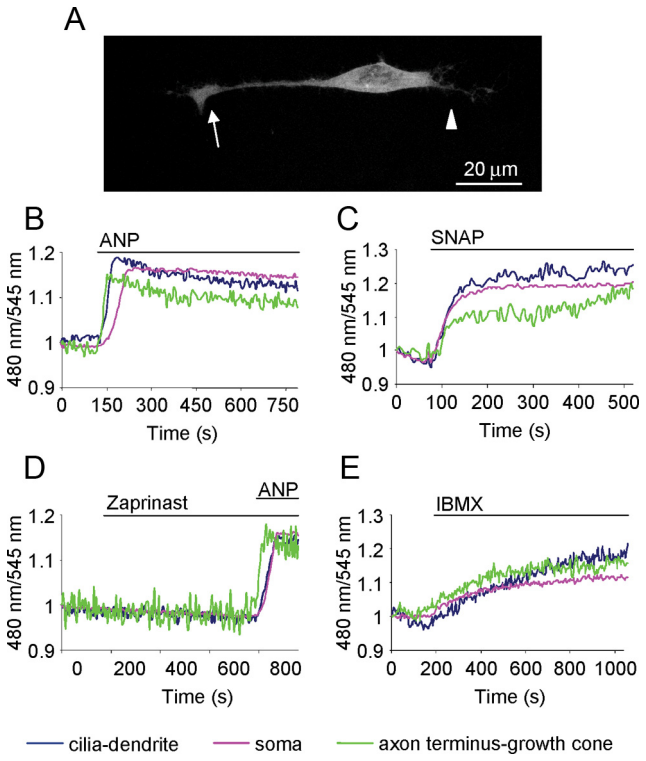


**Figure 2.** cGMP dynamics in OSN upon pharmacological stimuli. ***A***, Example of an OSN transfected with the sensor for cGMP. The fluorescence is distributed throughout the cytoplasm with the exclusion of the nucleus. Arrow, Axon terminus-growth cone; arrowhead, cilia-dendrite. Scale bar, 20 $\mu$m. ***B–E***, Normalized kinetics of fluorescence emission intensities (480/545 nm) recorded in cilia-dendrite, soma, and axon terminus-growth cone in OSNs transfected with the PKG-based sensor for cGMP and challenged with different stimuli, all bath applied via an application pipette positioned far away (~3 mm) from the cell, to obtain a homogeneous distribution of the stimuli in the bath. ***B–E***, ANP (1 $\mu$M) activator of mGC (***B***); SNAP (300 $\mu$M) NO donor, which activates sGC (***C***); zaprinast (250 $\mu$M), inhibitor of the cGMP-specific PDE-5 and subsequently with ANP (1 $\mu$M) (***D***); and IBMX (250 $\mu$M), nonselective inhibitor of PDEs (***E***). Neurons challenged only by Ringer's solution with or without the solvent (negative controls), did not present changes in fluorescence ratio, here and in all the subsequent treatments (data not shown). The regions of interest were drawn on the distal portion of the axon (axon terminus-growth cone), on the soma, and on the distal part of the dendrite (cilia-dendrite). Other conditions as in Materials and Methods. Blue line, CFP/YFP in cilia-dendrite; pink line, CFP/YFP in soma; green line, CFP/YFP in axon terminus-growth cone. Primary cultures of OSNs were used in all experiments.

### cGMP dynamics in OSNs upon physiological stimuli (odors)

We then investigated the spatial distribution and the temporal dynamics of cGMP in OSNs upon physiological stimulation (i.e., odors). Upon application of odor mixtures (1, 50, and 200 $\mu$M) (Fig. 3*A–C*, bath applied) a slow and sustained rise in cGMP in the entire neuron was observed. The higher concentration (200 $\mu$M) elicited cGMP responses very similar, in terms of kinetics, to those observed with the lower odor concentrations. At all the concentrations tested, the time for half-maximal response ($t_{1/2}$) was slightly, but significantly, faster at the cilia-dendrite and at the axon terminus-growth cone than at the soma (Fig. 3*A–C*). As expected, given the specificity of the OR expressed by each OSN, only a fraction of the neurons tested responded at the odor concentrations used. The higher concentration (200 $\mu$M) elicited $Ca^{2+}$ responses in a higher number of cells (1 $\mu$M, $n_{tot} = 62$, responsive cells = 5%; 50 $\mu$M, $n_{tot} = 50$, responsive cells = 12%; 200 $\mu$M, $n_{tot} = 67$, responsive cells = 30%). We then decided to use, in all the experiments that required odor stimulation, the concentration of 200 $\mu$M, a condition that increases the probability of finding responsive cells.

In a few cells, a variable lag phase (0.5–4 min) was observed between stimulus application and the onset of the response. The cGMP signal remained sustained for the entire duration of the experiment (at least 10 min, during which the stimulus, odor mixture, was present in the bath). However, the cGMP increase was reversible upon removal of the stimulus (bath applied for 5–7 min; $n = 6$) (Fig. 3*D*). Finally, the odor mixture was locally applied with a pipette directed to the axon terminus-growth cone (odor concentration in the pipette, 1 mM). Under these conditions, a rise in cGMP was observed exclusively at the axon terminus-growth cone ($n = 4$) (Fig. 3*E*) ($t_{1/2} = 1.5 \pm 0.2$ min), and no appreciable changes in signal were detected in the other compartments.

In a number of neurons ($n = 5$), we measured in the same cells the cGMP dynamics and the cytosolic $Ca^{2+}$ response (using the fluorescent indicator fura-2). One example is presented in Figure 3, *F* and *G*. For technical reasons, only the 380 nm component of the fura-2 indicator is reported (Fig. 3*G*). A decrease in the 380 nm component, as shown in Figure 3*G*, corresponds to an increase in the concentration of $Ca^{2+}$ in the cell. With no exception, when a rise in cGMP was observed a rise in $Ca^{2+}$ was also detected; and vice versa, no rise of $Ca^{2+}$ was observed in cells not responding to odors with a cGMP rise.

Nonspecific effects of odors on $Ca^{2+}$ and or cGMP levels were excluded because (1) the odor mix was without effect on the majority of OSNs tested (~70%), though the nonresponsive neurons presented a normal rise in $Ca^{2+}$ (Fig. 1*H*) or cGMP when subsequently tested with KCl (Fig. 3*H*); and (2) upon odor stimulation, no $Ca^{2+}$ or cGMP rise could be observed in HEK cells expressing the cGMP probe (Fig. 3*I*) and/or loaded with a fluorescent $Ca^{2+}$ indicator (fura-2; data not shown).

### Molecular mechanism underpinning cGMP increase

The question then arises as to the molecular mechanism underpinning the cGMP rise upon odor treatment. Given that the OSNs express both soluble and membrane-bound GCs, we first investigated which enzyme is activated upon OR stimulation.

We analyzed the ability of the inhibitor LY83583 to block sGC activity in living OSNs. Figure 4*A* shows that the rise of cGMP upon sGC stimulation by the NO donor SNAP was abolished by the sGC inhibitor LY83583 (Fig. 4*A*) ($n = 10$). However, the same neuron presented a prompt cGMP response when subsequently stimulated with SNAP alone, after washing away the inhibitor (Fig. 4*B*). To assess the role of sGC in the cGMP rise upon odor stimulation, OSNs were treated with odors in the presence of the inhibitor LY83583. In this condition, no cGMP increase was detected in the entire OSN (Fig. 4*C*). However, a rise in cGMP, in the same neuron, was observed after washing away the inhibitor and the subsequent application of odors (Fig. 4*D*).

It is known that sGCs are activated by gaseous ligands, NO, or CO according to the stage of development of the OSNs. NO is thought to be active only during development and in regenerating axons, while CO is active in adult OSNs (Roskams et al., 1994). Odor treatment in the presence of ZnPP9 (Fig. 4*E*), an inhibitor of HO, which synthesizes CO, caused a cGMP increase that was indistinguishable from that of controls (odors without ZnPP9). Again, the time to reach half-maximal concentration was faster at cilia-dendrite and axon terminus-growth cone than at the soma level ($n = 7$, $t_{1/2}$: cilia-dendrite = $2.9 \pm 0.7$ min; soma = $3.4 \pm 0.6$ min; axon terminus growth cone = $2.9 \pm 0.5$ min; *t* test $t_{1/2}$: cilia dendrite-soma, $^*p = 0.03$; axon terminus-growth cone-soma, $^*p = 0.04$; cilia dendrite-axon terminus-growth cone, $p = 0.9$). On the contrary, OSNs treated with odors

in the presence of 7-NI, an inhibitor of NOS, did not show any rise in cGMP level (Fig. 4*F*). The same neurons, after washing away the inhibitor, presented a positive response to the odor mixture applied subsequently (Fig. 4*G*) ($n = 5$).

The next question is to determine the mechanism coupling sGC to OR activation. The obvious candidate appears cAMP, which is synthesized upon odorant binding to their receptors. OSNs were thus treated with odors in the presence of the AC blocker SQ22536 (SQ22536 was incubated for 15 min before odor application). Under these conditions, odor treatment was unable to induce a cGMP rise. However, these same neurons, not responsive to odor in the presence of SQ22536, presented a prompt rise in cGMP after washing away the inhibitor and subsequent application of odors ($n = 5$) (Fig. 5*A*,*B*). To confirm that the cGMP increases are causally dependent on the cAMP rise, the OSNs transfected with the sensor for cGMP were treated with forskolin, a generic AC activator. After treatment with forskolin, an increase in cGMP was observed in all neurons (Fig. 5*C*) ($n = 5$, $t_{1/2}$: cilia-dendrite = 1.7 ± 0.2 min; soma = 2 ± 0.4 min; axon terminus-growth cone = 1.7 ± 0.4 min). Unlike the case of odors when only a fraction of the neurons tested responded with a cGMP rise, the vast majority (>90%) of the OSNs tested responded to forskolin.

The final and most important mechanistic question is to determine how cAMP can activate sGC activity. We first considered the possibility that the link between cAMP and sGC was PKA, the principal target of cAMP. However, OSNs treated with the odor mixture in the presence of a PKA inhibitor, H89 or KT5720, presented a rise in cGMP as in controls (i.e., neurons treated with odors only) (Fig. 5*D*) ($n = 10$, $t_{1/2}$: cilia-dendrite = 2.9 ± 0.5 min; soma = 3.4 ± 0.5 min; axon terminus growth cone = 2.7 ± 0.5 min; *t* test $t_{1/2}$: cilia dendrite-soma, $^{*}p = 0.04$; axon terminus-growth cone-soma, $^{**}p = 0.006$; cilia dendrite-axon terminus-growth cone, $p = 0.3$). The other potential target of cAMP is Epac, directly activated by cAMP (Bos, 2003). Epac exists as two isoforms, Epac 1 and Epac 2, whose expression is developmentally regulated. Epac 1 is expressed in embryonic and in early neonatal ages in the brain, spinal cord, and DRG, while Epac 2 is expressed in adulthood (Murray and Shewan, 2008). Since we are studying developing neurons, we checked the expression of Epac 1 in a primary culture of OSNs. Figure 5*E* shows that Epac 1 is homogeneously expressed in the entire OSN, including the axon terminus. Given that no selective inhibitor of Epac is commercially available, we treated OSNs with 8-CPT-2′-O-Me-cAMP, a selective and potent activator of Epac with no effect on PKA (Enserink et al., 2002). In addition, 8-CPT-2′-O-Me-cAMP is also known to be totally ineffective on cAMP-dependent ion channels (Bos, 2003). OSNs treated with this Epac activator presented a prompt rise in cGMP in the entire neuron (Fig. 5*F*) ($n = 8$, $t_{1/2}$: cilia-dendrite = 2.4 ± 0.3 min; soma = 2.8 ± 0.4 min; axon terminus-growth cone = 2.1 ± 0.4 min). Also in this case, as for the other pharmacological agents, the vast majority (>90%) of the tested neurons responded to the Epac activator.

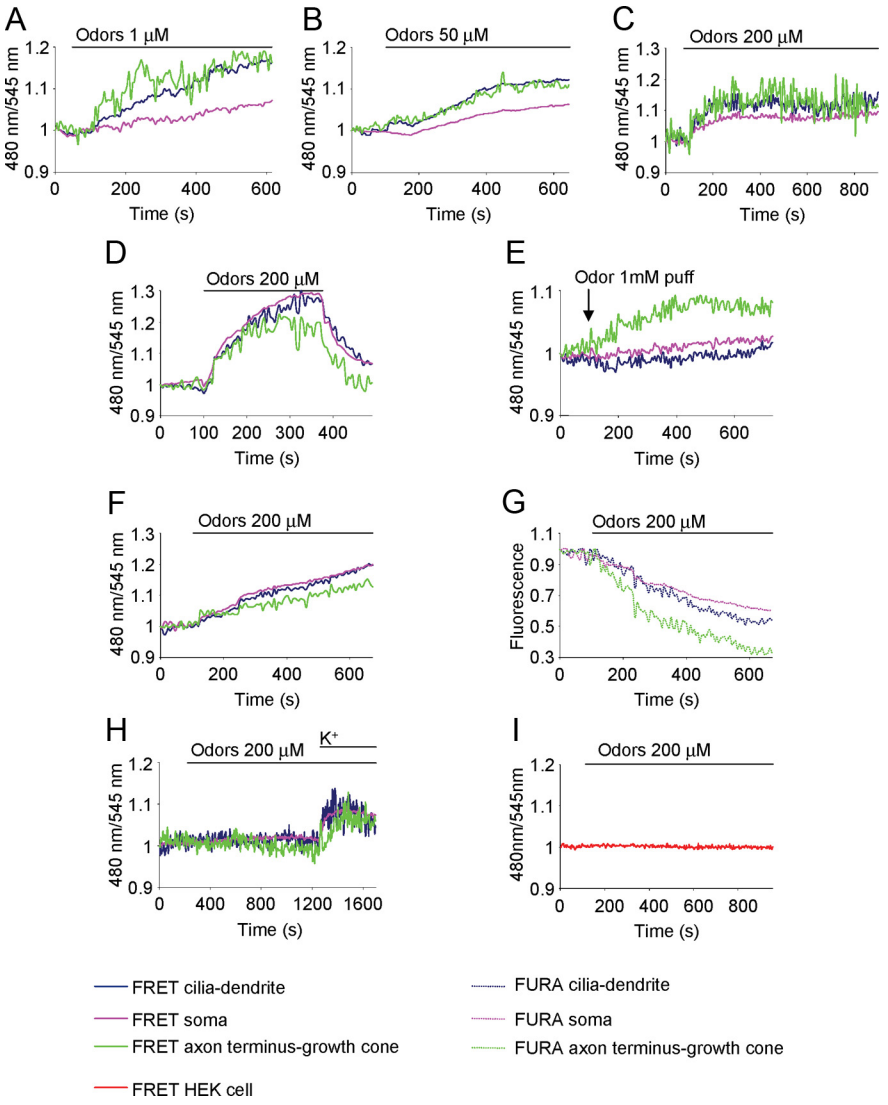


**Figure 3.** cGMP dynamics in OSNs upon physiological stimuli (odors). Conditions as in Figure 2. ***A–D***, Examples of the cGMP kinetics in OSNs treated with different concentrations of odors, bath applied: odors, 1 μM, $n = 3$, $t_{1/2}$ cilia-dendrite = 3 ± 0.3 min, soma = 4.2 ± 0.3 min, axon terminus-growth cone = 2.9 ± 0.2 min; *t* test $t_{1/2}$ cilia-dendrite-soma $^{*}p = 0.04$, axon terminus growth cone-soma $^{*}p = 0.02$, cilia dendrite-axon terminus growth cone $p = 0.8$ (***A***); odors, 50 μM, $n = 6$, $t_{1/2}$, cilia-dendrite = 2.7 ± 0.5 min, soma = 3.1 ± 0.5 min, axon terminus-growth cone = 2.4 ± 0.5 min, *t* test $t_{1/2}$ cilia dendrite-soma $^{*}p = 0.03$, axon terminus growth cone-soma $^{*}p = 0.02$, cilia dendrite-axon terminus growth cone $p = 0.4$ (***B***); odors, 200 μM, $n = 20$, $t_{1/2}$ cilia-dendrite = 2.2 ± 0.3 min; soma = 2.4 ± 0.4 min; axon terminus-growth cone = 2 ± 0.3 min; *t* test $t_{1/2}$ cilia dendrite-soma $^{*}p = 0.03$; axon terminus growth cone-soma $^{*}p = 0.02$, cilia dendrite-axon terminus growth cone $p = 0.3$ (***C***); and odors, 200 μM, bath applied for 5–7 min and then washed away (***D***); and cGMP rise in response to odors (1 mM in the pipette) locally applied with a glass pipette directed to the axon terminus (***E***). ***F***, ***G***, Examples of cGMP dynamics (FRET, 480/545 nm) (***F***) and calcium dynamics (fura-2, 380 nm component) (***G***) in the same neuron, transfected with the sensor for cGMP and loaded with fura-2, treated with odors (200 μM, bath applied). ***H***, Example of cGMP dynamics in an OSN not responsive to odors (200 μM, bath applied), but responsive to KCl (50 mM) subsequently bath applied. ***I***, example of cGMP dynamics in a HEK cell, not expressing OR (used as controls), treated with odors (200 μM, bath applied). Primary cultures of OSNs were used in all experiments. Solid lines represent the cGMP dynamics (***A–F***, ***H***); dotted lines denote $Ca^{2+}$ dynamics (***G***). Blue line, Cilia-dendrite; pink line, soma; green line, axon terminus-growth cone; red line, cGMP kinetics in HEK cell (***I***).

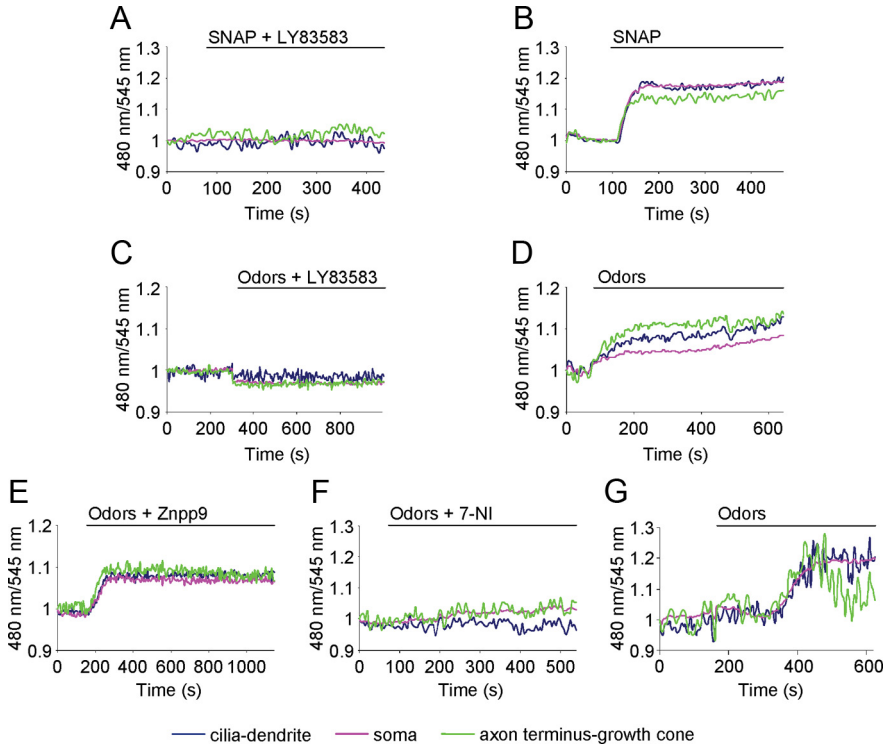


**Figure 4.** Molecular mechanism of GC activation. Conditions as in Figure 2. ***A***, ***B***, Examples of cGMP dynamics in the same OSN treated with the NO donor SNAP (300 $\mu$M, able to activate sGC) along with the sGC inhibitor LY83583 (10 $\mu$M) (***A***), and with SNAP after washing away the inhibitor LY83583 (***B***). ***C***, ***D***, The same OSN treated with odors (200 $\mu$M) in the presence of sGC inhibitor LY83583 (10 $\mu$M) (***C***), and with odors only (200 $\mu$M) after washing away the inhibitor LY83583 (***D***). ***E***, An OSN treated with odors (200 $\mu$M) in the presence of HO inhibitor ZnPP9 (10 $\mu$M). ***F***, ***G***, the same OSN treated with odors (200 $\mu$M) in the presence of NOS inhibitor 7-NI (30 $\mu$M) (***F***), and with odors only (200 $\mu$M) after washing away the inhibitor 7-NI (***G***). Stimuli were all bath applied. Blue line, Cilia-dendrite; pink line, soma; green line, axon terminus-growth cone. Primary cultures of OSNs were used in all experiments.

Given that NOS is known to be activated by $Ca^{2+}$-calmodulin, the simplest explanation for the above results is that NO production (and thus sGC activation) would be dependent on cAMP-triggered $Ca^{2+}$ increases [through cyclic nucleotide-gated (CNG) channels and other mechanisms; see below]. Indeed, a $Ca^{2+}$ increase, as induced by depolarizing the neurons with KCl (50 mM), resulted in a clear increase in cGMP in the OSN (Fig. 5*G*) ($n = 4$, $t_{1/2}$: cilia-dendrite = 2.6 ± 0.4 min; soma = 2.9 ± 0.3 min; axon terminus-growth cone = 2.5 ± 0.3 min).

We next challenged the OSNs with odors while bathed in a $Ca^{2+}$-free Ringer's solution (supplemented with 1 mM EGTA), a condition that prevents any influx of $Ca^{2+}$ from the medium. In these conditions, however, a clear rise in cGMP was still observed, indicating that odors may also cause the release of $Ca^{2+}$ from intracellular stores. Time to reach half-maximal concentration ($t_{1/2}$) was longer, although not significantly, with respect to that observed in OSNs in normal Ringer's solution (Fig. 5*H*) ($n = 12$, $t_{1/2}$: cilia-dendrite = 3.2 ± 0.6 min; soma = 3.7 ± 0.7 min; axon terminus-growth cone = 3.1 ± 0.6 min; *t* test $t_{1/2}$: cilia dendrite-soma, $^{*}p = 0.01$; axon terminus-growth cone-soma, $^{**}p = 0.005$; cilia dendrite-axon terminus-growth cone, $p = 0.4$). Furthermore, the number of responsive neurons in $Ca^{2+}$-free solution was slightly lower (22 vs 30%) than in normal Ringer's solution.

These results suggested that the release of $Ca^{2+}$ from intracellular stores is sufficient, in most cells, to activate NOS and thus to cause a rise of cGMP.

How could Epac activation induce $Ca^{2+}$ mobilization from stores? One likely possibility is via the production of $IP_3$. Indeed, among the targets of Epac there is PLCε, whose activation results in diacylglycerol and $IP_3$ formation and subsequent release of $Ca^{2+}$ from stores (Schmidt et al., 2001; Bos, 2003). To test this possibility, OSNs were loaded with the fluorescent $Ca^{2+}$ indicator fura-2 and then challenged with forskolin (25 $\mu$M) (Fig. 6*A*) ($n = 11$), with the Epac activator 8-CPT-2′-O-Me-cAMP (30 $\mu$M) (Fig. 6*B*) ($n = 10$), or with odors ($n = 3$, data not shown) while bathed in a $Ca^{2+}$-free Ringer's solution (supplemented with 1 mM EGTA). As shown in the Figure 6, a slow and sustained rise in cytosolic $Ca^{2+}$ was observed under these conditions. In a few cells, a lag phase between the application of the stimulus and the onset of the response was observed.

The most important $IP_3$-sensitive $Ca^{2+}$ store in nonmuscle cells is the endoplasmic reticulum (ER). To evaluate the ER distribution in the OSNs, the cells were immunostained with antibodies against two canonical markers of the organelle, SERCA and calreticulin (Rizzuto and Pozzan, 2006). As shown in Figure 6, *C* and *D*, both antibodies decorated a delicate reticular structure in dendrite, soma, and axon.

To directly evaluate the release of $Ca^{2+}$ from the ER, primary cultures of OSNs were transiently transfected with a genetically encoded $Ca^{2+}$ sensor, targeted to the ER lumen, D1ER (Rudolf et al., 2006). OSN transfected with D1ER (Fig. 6*E*) presented a clear diffuse fluorescence in dendrite, soma, and axon resembling the labeling observed in OSNs immunostained with antibodies against SERCA and calreticulin (Fig. 6*C*,*D*). Changes in $[Ca^{2+}]$ER result in modification of FRET in D1ER and can be conveniently monitored by the changes of the YFP/CFP fluorescence emission ratio (545/480 nm). A drop in $[Ca^{2+}]$ER is associated to a reduction of the YFP/CFP fluorescence emission ratio (545/480 nm). As shown in Figure 6*F*, OSNs transfected with D1ER and challenged, in normal $Ca^{2+}$-containing medium, with the Epac activator (30 $\mu$M, $n = 6$) presented a slow and sustained drop in $[Ca^{2+}]$ER (corresponding to $Ca^{2+}$ release from stores) in dendrite, soma, and axon terminus. When OSNs, transfected with D1ER, were treated with odors (200 $\mu$M), again a slow and prolonged reduction in $[Ca^{2+}]$ER signal was observed in the entire OSN (Fig. 6*G*) ($n = 8$). When the same experiments were performed in $Ca^{2+}$-free Ringer's solution supplemented with EGTA (1 mM), the $[Ca^{2+}]$ER drop was similar or larger to the one observed in $Ca^{2+}$-containing medium.

Most important from a mechanistic point of view, the $Ca^{2+}$ release from the ER was abolished when responsive neurons were subsequently rechallenged with odors in the presence of the inhibitor of PLCε, U73122 (30 $\mu$M, incubated for 15 min before odor application; $n = 6$) (Fig. 6*H*). To exclude the possibility that the lack of response to odors in the presence of the inhibitor of PLCε was due to desensitization of the OR after the first stimulation, the odor mix was

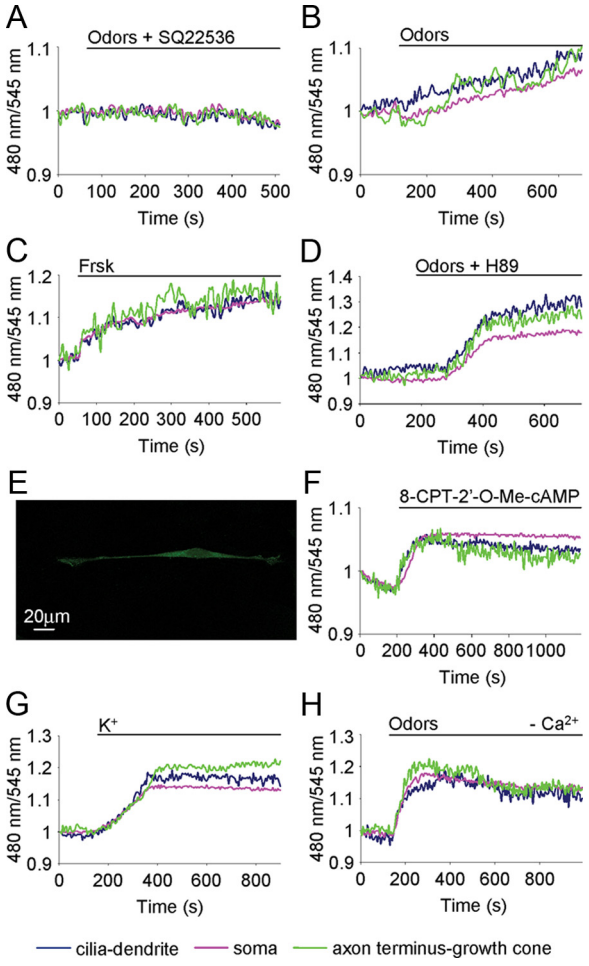


**Figure 5.** Molecular mechanism underpinning cGMP rise. Conditions as in Figure 2. ***A***, ***B***, Examples of the spatiotemporal dynamics of cGMP in the same OSN treated with odors (200 $\mu$M) in presence of AC inhibitor SQ22536 (30 $\mu$M) (***A***) and with odors only (200 $\mu$M) after washing away the inhibitor SQ22356 (***B***). ***C***, ***D***, OSNs treated with Frsk (25 $\mu$M), AC activator (***C***), and odors (200 $\mu$M) in the presence of the PKA inhibitor H89 (10 $\mu$M) (***D***). ***E***, Example of an OSN immunopositive for Epac1. The immunofluorescence is present in the entire neuron. Scale bar, 20 $\mu$m. ***F–H***, Examples of cGMP dynamics in OSNs treated with Epac activator 8-CPT-2′-O-Me-cAMP (30 $\mu$M) (***F***), KCl (50 mM) (***G***), and odors (200 $\mu$M), in a $Ca^{2+}$-free Ringer's solution (***H***). Stimuli were all bath applied. Blue line, Cilia-dendrite; pink line, soma; green line, axon terminus-growth cone. Primary cultures of OSNs were used in all experiments.

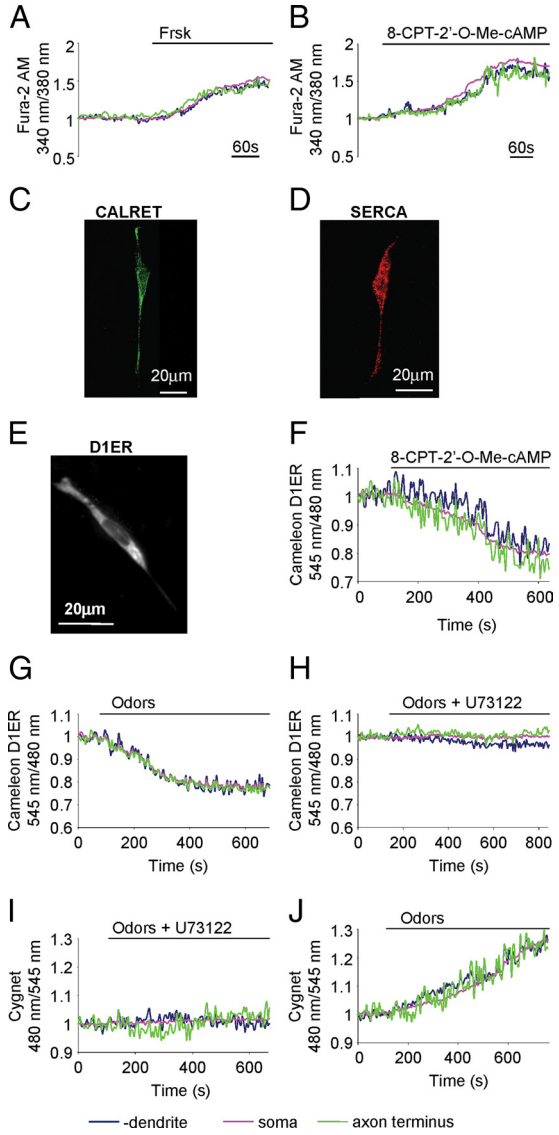


**Figure 6.** Mobilization of $Ca^{2+}$ from stores and cGMP synthesis. ***A***, ***B***, Normalized fluorescence ratio changes (340/380 nm) in OSNs loaded with fura-2 and challenged with Frsk (25 $\mu$M) AC activator (***A***) and Epac activator 8-CPT-2′-O-Me-cAMP (30 $\mu$M) (***B***). ***C***, ***D***, Example of OSNs immunopositive for two canonical ER markers: calreticulin (***C***) and SERCA (***D***). ***E***, Example of an OSN transiently transfected with the genetically encoded $Ca^{2+}$ sensor, targeted to the ER lumen D1ER. ***F–H***, $Ca^{2+}$ dynamics in OSNs transiently transfected with D1ER and treated with: Epac activator 8-CPT-2′-O-Me-cAMP (30 $\mu$M) (***F***). ***G***, ***H***, The same neuron, treated with odors (200 $\mu$M) (***G***) and with odors in the presence of the PLC$\varepsilon$ inhibitor U73122 (30 $\mu$M) (***H***). ***I***, ***J***, cGMP dynamics in the same OSN transiently transfected with the sensor for cGMP, Cygnet, and challenged with odors (200 $\mu$M) in the presence of the PLC$\varepsilon$ inhibitor U73122 (30 $\mu$M) (***I***) and with odors (200 $\mu$M) only, and after washing away the inhibitor (***J***). Stimuli were all bath applied. In ***A***, ***B***, ***I***, and ***J***, OSNs were bathed in $Ca^{2+}$-free Ringer's solution. Blue line, Dendrite; pink line, soma; green line, axon terminus. Scale bar, 20 $\mu$m. Primary culture of OSNs were used in all experiments.

first applied in the presence of the inhibitor and subsequently after washing away the inhibitor. No release of $Ca^{2+}$ was ever detected in the presence of the inhibitor, whereas it was observed upon removal of the blocker (data not shown).

To directly evaluate the role of $Ca^{2+}$ release from stores, via PLC$\varepsilon$, in cGMP synthesis, OSNs transfected with the sensor for cGMP, Cygnet (while bathed in $Ca^{2+}$-free Ringer's solution, supplemented with EGTA 1 mM) were treated with odors in the presence of the inhibitor of PLC$\varepsilon$. Under these conditions, no rise of cGMP could be detected. However, after washing away the inhibitor, the same neurons presented a clear rise in cGMP ($n = 5$) (Fig. 6*I–J*).

### cGMP action at the nuclear level

cGMP can exert its action locally at the cilia-dendrite and at the axon terminus where it is produced, but, since it is involved in long-term response to odors, it may also act at the nuclear level, regulating gene expression (e.g., via P-CREB). To test this hypothesis, we treated OSNs with 8Br-cGMP (bath applied), a membrane-permeable analog of cGMP, and we looked for P-CREB at the nuclear level ($n = 4$ cultures). Upon treatment with 8Br-cGMP, OSNs presented an increased immunopositive labeling for P-CREB in the nuclei (Fig. 7*A–C*) (P-CREB level, controls vs treated, *t* test, $^{***}p < 0.001$).

The question then arises as to the physiological significance of these findings *in vivo*. To assess whether the cGMP produced upon activation of the OR at the axon terminus can exert its action not only locally, but also at the nuclear level, 8Br-cGMP

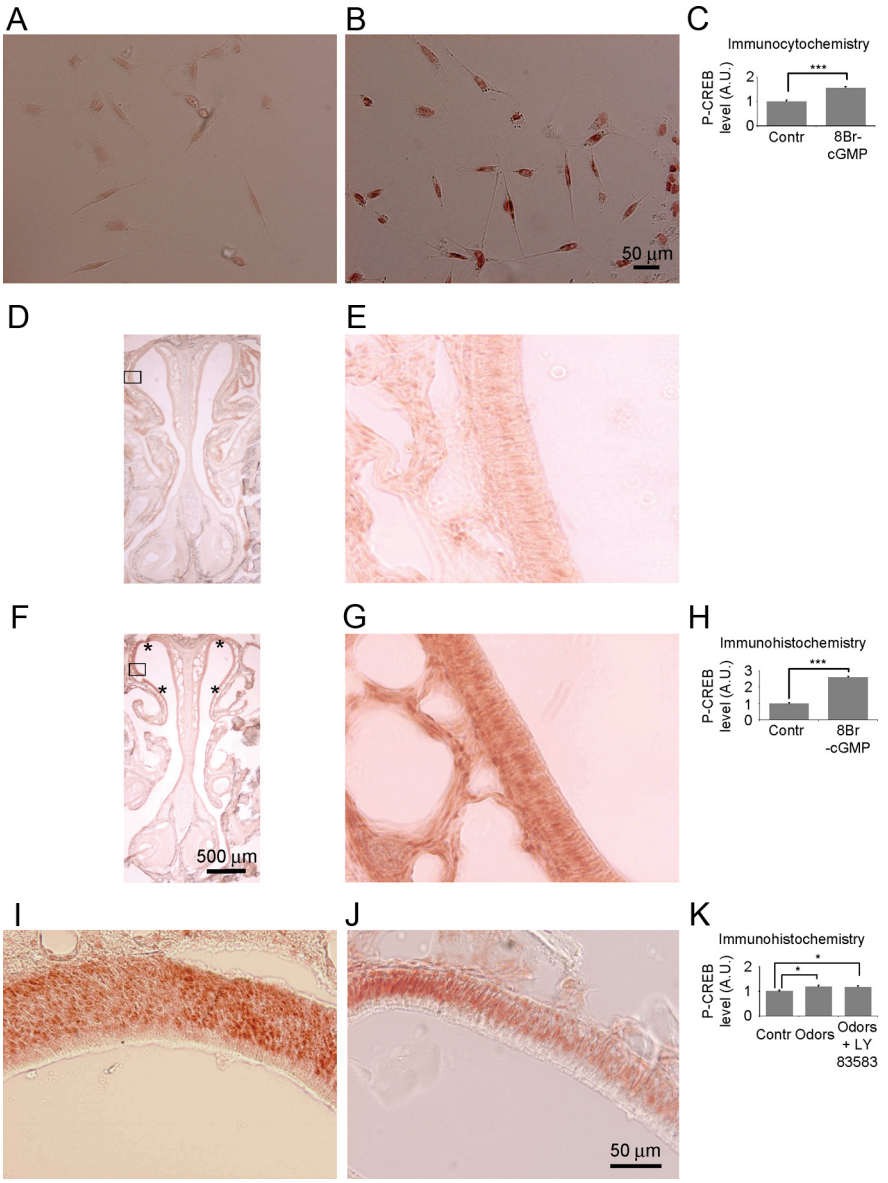


**Figure 7.** Phosphorylation of CREB in OSNs. ***A***, ***B***, Primary culture of OSNs immunostained with an antibody against P-CREB in controls (i.e., OSNs treated with Ringer's solution) (***A***) and after treatment with the membrane-permeable cGMP analog 8Br-cGMP (50 $\mu$M) (***B***). ***C***, Summary of the experiments performed in ***A*** and ***B***, normalized P-CREB level (***$p < 0.001$). ***D***, ***F***, Coronal sections of the olfactory epithelium immunostained with an antibody against P-CREB after application of Ringer's solution (controls) (***D***) and 8-BrcGMP (250 $\mu$M) (***F***) at the axon terminus of the OSNs in the olfactory bulb *in vivo*. Asterisks signify the portion of the epithelium with increased P-CREB levels. Scale bars: ***D***, ***F***, 500 $\mu$m; ***E***, ***G***, higher magnification (20×) of the epithelium indicated in the squares in ***D*** and ***F***, respectively. ***H***, Summary of experiments in ***D–G*** (normalized P-CREB level, ***$p < 0.001$). ***I***, ***J***, Portions of coronal sections of the olfactory epithelium immunostained with an antibody against P-CREB, after odors (1 mM) (***I***) and odors (1 mM) in the presence of the sGC inhibitor LY83583 (250 $\mu$M) were applied at the axon terminus of the OSNs in the olfactory bulb *in vivo*. ***K***, Summary of experiments performed in ***I*** and ***J***, normalized P-CREB level, controls versus odors, *$p = 0.02$; controls versus odors + LY83583, *$p = 0.03$; odors versus odors + LY83583, $p = 0.8$. A.U, Arbitrary units. Scale bar, 50 $\mu$m.

was applied to the olfactory bulbs *in vivo*. We found that within 30–40 min from 8Br-cGMP application it was possible to detect a large increase in P-CREB in the nuclei of OSNs, in a small dorsal portion (14%), only in few slices of the epithelium, approximately corresponding to the dorsal portion (20%) of the OB bathed with 8Br-cGMP (Fig. 7*D–H*) ($n = 4$ mice, P-CREB level, controls vs 8Br-cGMP, *t* test, ***$p < 0.001$). Finally, and most relevant, local odor application on the bulbs was followed by the presence of P-CREB in the OSN nuclei within 30–40 min (Fig. 7*I*) ($n = 4$ mice, P-CREB level, controls vs odors, *t* test, *$p = 0.02$). However, when odors were applied on the bulbs in presence of the sGC inhibitor LY83583 ($n = 5$ mice), we could still reveal the presence of P-CREB in the nuclei, as shown in Figure 7, *J* and *K* (P-CREB level, controls vs odors + LY83583, *t* test, *$p = 0.03$; P-CREB level, odors vs odors + LY83583, $p = 0.8$). Together, these results indicate that a rise in cGMP is sufficient, but not necessary, to induce phosphorylation of CREB at the nuclear level.

## Discussion

In this study, we analyzed the spatial and temporal kinetics of cGMP in living OSNs transfected with a genetically encoded sensor for cGMP, and we found that upon pharmacological and physiological stimuli a rise in cGMP is observed in the entire OSN.

Upon stimulation with ANP, an activator of mGCs, or SNAP, a NO donor capable of activating sGCs, a prompt and sustained increase in cGMP, with no lag phase between stimulus application and the starting point of the response, was observed in the entire neuron. The time to reach half-maximal response was faster at the axon terminus-growth cone and at the cilia-dendrite than at the soma, only in neurons treated with ANP. These results are likely to reflect the different distribution of the two forms of guanylyl cyclases.

The lack of zaprinast effect on cGMP under basal conditions suggests that, although the drug is a potent inhibitor of cGMP-PDE, other PDEs (i.e., PDE 1 and 2) play a role in the hydrolysis of cGMP. This can also explain the lack of a larger response to ANP added subsequently to zaprinast. Alternatively, or in addition, it may indicate that the basal activity of the GCs is very low. As to the effect of IBMX on cGMP level, this most likely depends on the cAMP rise induced by the drug (Maritan et al., 2009), followed by a rise in $Ca^{2+}$ and NOS activation (see below).

The results with zaprinast are in contrast with those obtained in previous studies (Moon et al., 1998, 2005). The reason for this discrepancy is presently unclear, and it is likely due to the different preparations and/or to the different techniques used (radioimmunoassay in tissue extracts).

When OSNs were challenged with a mixture of odorants, a slow and sustained increase in cGMP in the entire neuron was observed. The time to reach half-maximal concentration ($t_{1/2}$) was faster at the cilia-dendrite and at the axon terminus-growth cone than at the soma level. This latter observation demonstrates that in the axon terminus-growth cone the cGMP rise does not derive from diffusion of cGMP produced at the cilia-dendrite level. This conclusion was confirmed by local stimulation of the

OR at the axon terminus-growth cone with odors focally applied with a pipette. In this case, the cGMP increase was detected solely at the axon terminus-growth cone.

As to the rise of cGMP at the soma upon odor stimulation, the kinetics of the cGMP signal we observed seems consistent with the diffusion of cGMP from other compartments, although we cannot exclude, in OSNs *in vitro*, a low expression of the OR at the soma. Alternatively, or in addition, the $Ca^{2+}$ increase coupled to odor-OR activation at the cilia-dendrite and at the axon terminus-growth cone, may diffuse and cause NOS activation and cGMP production directly at the soma.

The main question addressed here is the mechanism underlying the cGMP generation in the OSN, a problem investigated previously by various groups with contradictory conclusions. We found that odors give rise to the cGMP increase by sGC activation via NO. Due to the temporal pattern of expression, it has been suggested that NO-cGMP (Roskams et al., 1994; Kafitz et al., 2000; Chen et al., 2004) plays a role during development and in regeneration while CO-cGMP is involved in the setting of long-term odor response in adult OSNs (Verma et al., 1993; Ingi and Ronnett, 1995). The local synthesis of cGMP that we found in developing axons is consistent with this hypothesis. In particular, the odor-dependent cGMP increases were completely inhibited by NOS blockade and totally insensitive to HO inhibition. It needs stressing that OSNs are constantly regenerating *in vivo*, and accordingly there is always a subpopulation of developing neurons.

The synthesis of cGMP at the axon terminus is of relevance since in other systems it has been shown that the cAMP/cGMP ratio is critical in directing the axon in its navigation (Nishiyama et al., 2003). In addition, Murphy and Isaacson (2003), on the basis of indirect evidence, suggested that cGMP and cAMP can modulate synaptic transmission between OSNs and postsynaptic cells; thus, they hypothesized that these two cyclic nucleotides could contribute to axon pathfinding.

As to the coupling between OR and NOS/sGC, some evidence supports the idea that cAMP and $Ca^{2+}$ play essential roles, in particular the following: (1) a cAMP increase is a prerequisite for odor-dependent cGMP synthesis, since, in the presence of AC inhibitors, odors were unable to increase cGMP; and (2) pharmacological increases in cAMP, as induced by either forskolin or IBMX, result in clear increases in cGMP. Furthermore, we demonstrate that the link between cAMP and NOS/sGC is represented by a cytoplasmic $Ca^{2+}$ increase, generated by plasma membrane $Ca^{2+}$ channel activation and $Ca^{2+}$ released from stores controlled by the cAMP-binding protein Epac. This scheme is consistent with the well known $Ca^{2+}$-calmodulin dependency of neuronal NOS (Breer and Shepherd, 1993), with the activation of $Ca^{2+}$ influx through CNG channels by cAMP, and with the finding that a rise in cytosolic $Ca^{2+}$, elicited solely by $K^+$ depolarization, results in an increase in cGMP.

The link between $Ca^{2+}$ and cGMP via the NOS-sGC activation is further supported by the parallel dynamics of the two signals, as clearly shown in the FRET and fura-2 experiments (Fig. 3). Indeed, the sustained cGMP signal reflects the sustained $Ca^{2+}$ signal, suggesting a prolonged $Ca^{2+}$-dependent activation of NOS-sGC. After washing away the stimulus, both the $Ca^{2+}$ and cGMP signals were reversible (Figs. 1, 3).

The contribution of the $Ca^{2+}$ release from stores in OSN signaling is still controversial, and different results have been obtained in different preparations (Zufall et al., 2000; Otsuguro et al., 2005). Here we found that cAMP, produced upon forskolin or odor administration in $Ca^{2+}$-free medium, can induce an increase in cytosolic $Ca^{2+}$. This $Ca^{2+}$ signal is due to $Ca^{2+}$ release from the ER, as we directly demonstrated in OSNs transfected with a genetically encoded $Ca^{2+}$ sensor specifically targeted to the ER lumen (Fig. 6*F*,*G*). Furthermore, we show that the link between cAMP-Epac activation and the release of $Ca^{2+}$ from the ER is represented by PLC$\varepsilon$, as demonstrated by the absence of $Ca^{2+}$ release in OSNs treated with odors in the presence of the inhibitors of the latter enzyme (Fig. 6*H*).

cGMP has always been associated with long-term responses, such as odor adaptation (Zufall and Leinders-Zufall, 1997, 1998), neuronal development and regeneration (Roskams et al., 1994; Chen et al., 2003), and olfactory imprinting (Dittman et al., 1997). In these long-term processes, cGMP may also be involved in regulating gene expression (i.e., via CREB phosphorylation). Here we show that 8 Br-cGMP induces phosphorylation of CREB in OSNs not only *in vitro* (Moon et al., 1999), but also *in vivo*, when the cGMP analog is applied to the OB. Phosphorylation of CREB, due to 8Br-cGMP is likely due to (1) cytosolic $Ca^{2+}$ rise, due to cGMP activation of CNG channels at the axon terminus (Murphy and Isaacson, 2003), and (2) PKG activation and translocation into the nucleus (Gudi et al., 1997). Interestingly, we also demonstrated that odors applied on the OB in live animals can induce P-CREB in the nuclei of OSNs. However, in this latter case, the phosphorylation of CREB did not depend critically on cGMP production, since P-CREB formation in the nuclei of OSNs was still observed upon odor treatment in the presence of the sGC inhibitor LY83583. These results can be explained by the presence of several mechanisms potentially involved in phosphorylation of CREB, upon OR activation at the glomeruli level. The increases of cAMP and $Ca^{2+}$, through CNG channels and through voltage-operated $Ca^{2+}$ channels, result in a rise of nuclear $Ca^{2+}$ that can be followed by phosphorylation of CREB by CaM kinases. $Ca^{2+}$ may also diffuse from the synapse to the cell body through a regenerative mechanism (i.e., $Ca^{2+}$-induced $Ca^{2+}$ release) (Rizzuto and Pozzan, 2006). Furthermore, in a previous article (Maritan et al., 2009), we found that focal application of odors at the axon terminus in cultured neurons was followed by nuclear translocation of the catalytic subunit of PKA, which can in turn induce CREB phosphorylation. Thus, diffusion of the catalytic subunit of PKA could be another possibility. The different scenarios presented here suggest that both PKA and $Ca^{2+}$ are likely to be involved in the phosphorylation of CREB.

Together, the present data suggest that cGMP, although not involved in initial stimulus detection events, due to the slow kinetics, could play numerous functions in OSNs in the settings of long-term cellular responses coupled to OR activation. On the one hand, the local production of cGMP at the axon terminus-growth cone may be of relevance in axon targeting/transmitter release, and, on the other hand, by activating CREB phosphorylation at the nuclear level, it could regulate expression of genes independently, or in synergy, with cAMP and $Ca^{2+}$ (Imai and Sakano, 2007). Therefore, we suggest that not only the OR-derived signal, cAMP (Imai et al., 2006), but also cGMP could play a key role in axon targeting acting both locally and at the nuclear level. In this scenario, the presence of Epac in the signaling pathway leading to cGMP synthesis appears particularly relevant, since in other systems it has been shown that Epac is involved, along with cyclic nucleotides, in neurite outgrowth and turning (Murray et al., 2009).

## References


Bhandawat V, Reisert J, Yau KW (2005) Elementary response of olfactory receptor neurons to odorants. Science 308:1931–1934.

Bhandawat V, Reisert J, Yau KW (2010) Signaling by olfactory receptor neurons near threshold. Proc Natl Acad Sci U S A 107:18682–18687.

Boehning D, Moon C, Sharma S, Hurt KJ, Hester LD, Ronnett GV, Shugar D, Snyder SH (2003) Carbon monoxide neurotransmission activated by CK2 phosphorylation of heme oxygenase-2. Neuron 40:129–137.

Bos JL (2003) Epac: a new cAMP target and new avenues in cAMP research. Nat Rev Mol Cell Biol 4:733–738.

Bozza TC, Kauer JS (1998) Odorant response properties of convergent olfactory receptor neurons. J Neurosci 18:4560–4569.

Bozza T, Feinstein P, Zheng C, Mombaerts P (2002) Odorant receptor expression defines functional units in the mouse olfactory system. J Neurosci 22:3033–3043.

Breer H, Shepherd GM (1993) Implications of the NO/cGMP system for olfaction. Trends Neurosci 16:5–9.

Chen J, Tu Y, Moon C, Nagata E, Ronnett GV (2003) Heme oxygenase-1 and heme oxygenase-2 have distinct roles in the proliferation and survival of olfactory receptor neurons mediated by cGMP and bilirubin, respectively. J Neurochem 85:1247–1261.

Chen J, Tu Y, Moon C, Matarazzo V, Palmer AM, Ronnett GV (2004) The localization of neuronal nitric oxide synthase may influence its role in neuronal precursor proliferation and synaptic maintenance. Dev Biol 269:165–182.

Dellacorte C, Kalinoski DL, Huque T, Wysocki L, Restrepo D (1995) NADPH diaphorase staining suggests localization of nitric oxide synthase within mature vertebrate olfactory neurons. Neuroscience 66:215–225.

Dittman AH, Quinn TP, Nevitt GA, Hacker B, Storm DR (1997) Sensitization of olfactory guanylyl cyclase to a specific imprinted odorant in Coho salmon. Neuron 19:381–389.

Dunn TA, Storm DR, Feller MB (2009) Calcium-dependent increases in protein kinase-A activity in mouse retinal ganglion cells are mediated by multiple adenylate cyclases. PLoS One 4:e7877.

Enserink JM, Christensen AE, de Rooij J, van Triest M, Schwede F, Genieser HG, Døskeland SO, Blank JL, Bos JL (2002) A novel Epac-specific cAMP analogue demonstrates independent regulation of Rap1 and ERK. Nat Cell Biol 4:901–906.

Gudi T, Lohmann SM, Pilz RB (1997) Regulation of gene expression by cyclic GMP-dependent protein kinase requires nuclear translocation of the kinese: identification of the nuclear localization signal. Mol Cell Biol 17:5244–5254.

Honda A, Adams SR, Sawyer CL, Lev-Ram V, Tsien RY, Dostmann WR (2001) Spatiotemporal dynamics of guanosine 3′,5′-cyclic monophosphate revealed by a genetically encoded, fluorescent indicator. Proc Natl Acad Sci U S A 98:2437–2442.

Imai T, Sakano H (2007) Roles of odorant receptors in projecting axons in the mouse olfactory system. Curr Opin Neurobiol 17:507–515.

Imai T, Suzuki M, Sakano H (2006) Odorant receptor-derived cAMP signals direct axonal targeting. Science 314:657–661.

Ingi T, Ronnett GV (1995) Direct demonstration of a physiological role for carbon monoxide in olfactory receptor neurons. J Neurosci 15:8214–8222.

Juilfs DM, Fülle HJ, Zhao AZ, Houslay MD, Garbers DL, Beavo JA (1997) A subset of olfactory neurons that selectively express cGMP-stimulated phosphodiesterase (PDE2) and guanylyl cyclase-D define a unique olfactory signal transduction pathway. Proc Natl Acad Sci U S A 94:3388–3395.

Kafitz KW, Leinders-Zufall T, Zufall F, Greer CA (2000) Cyclic GMP evoked calcium transients in olfactory receptor cell growth cones. Neuroreport 11:677–681.

Kroner C, Boekhoff I, Lohmann SM, Genieser HG, Breer H (1996) Regulation of olfactory signalling via cGMP-dependent protein kinase. Eur J Biochem 236:632–637.

Leinders-Zufall T, Cockerham RE, Michalakis S, Biel M, Garbers DL, Reed RR, Zufall F, Munger SD (2007) Contribution of the receptor guanylyl cyclase GC-D to chemosensory function in the olfactory epithelium. Proc Natl Acad Sci U S A 104:14507–14512.

Liu N, Shields CB, Roisen FJ (1998) Primary culture of adult mouse olfactory receptor neurons. Exp Neurol 151:173–183.

Lohof AM, Quillan M, Dan Y, Poo MM (1992) Asymmetric modulation of cytosolic cAMP activity induces growth cone turning. J Neurosci 12:1253–1261.

Lucas KA, Pitari GM, Kazerounian S, Ruiz-Stewart I, Park J, Schulz S, Chepenik KP, Waldman SA (2000) Guanylyl cyclases and signaling by cyclic GMP. Pharmacol Rev 52:375–414.

Lugnier C (2006) Cyclic nucleotide phosphodiesterase (PDE) superfamily: a new target for the development of specific therapeutic agents. Pharmacol Ther 109:366–398.

Malnic B, Hirono J, Sato T, Buck LB (1999) Combinatorial receptor codes for odors. Cell 96:713–723.

Maritan M, Monaco G, Zamparo I, Zaccolo M, Pozzan T, Lodovichi C (2009) Odorant receptors at the growth cone are coupled to localized cAMP and Ca2+ increases. Proc Natl Acad Sci U S A 106:3537–3542.

Menini A (1999) Calcium signalling and regulation in olfactory neurons. Curr Opin Neurobiol 9:419–426.

Moon C, Jaberi P, Otto-Bruc A, Baehr W, Palczewski K, Ronnett GV (1998) Calcium-sensitive particulate guanylyl cyclase as a modulator of cAMP in olfactory receptor neurons. J Neurosci 18:3195–3205.

Moon C, Sung YK, Reddy R, Ronnett GV (1999) Odorants induce the phosphorylation of the cAMP response element binding protein in olfactory receptor neurons. Proc Natl Acad Sci U S A 96:14605–14610.

Moon C, Simpson PJ, Tu Y, Cho H, Ronnett GV (2005) Regulation of intracellular cyclic GMP levels in olfactory sensory neurons. J Neurochem 95:200–209.

Murphy GJ, Isaacson JS (2003) Presynaptic cyclic nucleotide-gated ion channels modulate neurotransmission in the mammalian olfactory bulb. Neuron 37:639–647.

Murray AJ, Shewan DA (2008) Epac mediates cyclic AMP-dependent axon growth, guidance and regeneration. Mol Cell Neurosci 38:578–588.

Murray AJ, Peace AG, Shewan DA (2009) cGMP promotes neurite outgrowth and growth cone turning and improves axon regeneration on spinal cord tissue in combination with cAMP. Brain Res 1294:12–21.

Nishiyama M, Hoshino A, Tsai L, Henley JR, Goshima Y, Tessier-Lavigne M, Poo MM, Hong K (2003) Cyclic AMP/GMP-dependent modulation of Ca2+ channels sets the polarity of nerve growth-cone turning. Nature 423:990–995.

Otsuguro K, Gautam SH, Ito S, Habara Y, Saito T (2005) Characterization of forskolin-induced Ca2+ signals in rat olfactory receptor neurons. J Pharmacol Sci 97:510–518.

Rizzuto R, Pozzan T (2006) Microdomains of intracellular $Ca^{2+}$: molecular determinants and functional consequences. Physiol Rev 86:369–408.

Ronnett GV, Hester LD, Snyder SH (1991) Primary culture of neonatal rat olfactory neurons. J Neurosci 11:1243–1255.

Roskams AJ, Bredt DS, Dawson TM, Ronnett GV (1994) Nitric oxide mediates the formation of synaptic connections in developing and regenerating olfactory receptor neurons. Neuron 13:289–299.

Rudolf R, Magalhães PJ, Pozzan T (2006) Direct in vivo monitoring of sarcoplasmic reticulum Ca2+ and cytosolic cAMP dynamics in mouse skeletal muscle. J Cell Biol 173:187–193.

Schmidt M, Evellin S, Weernink PA, von Dorp F, Rehmann H, Lomasney JW, Jakobs KH (2001) A new phospholipase-C-calcium signalling pathway mediated by cyclic AMP and a Rap GTPase. Nat Cell Biol 3:1020–1024.

Touhara K, Sengoku S, Inaki K, Tsuboi A, Hirono J, Sato T, Sakano H, Haga T (1999) Functional identification and recostitution of an odorant receptor in single olfactory neurons. Proc Natl Acad Sci U S A 96:4040–4045.

Verma A, Hirsch DJ, Glatt CE, Ronnett GV, Snyder SH (1993) Carbon monoxide: a putative neural messenger. Science 259:381–384.

Zufall F, Leinders-Zufall T (1997) Identification of a long-lasting form of odor adaptation that depends on the carbon monoxide/cGMP second-messenger system. J Neurosci 17:2703–2712.

Zufall F, Leinders-Zufall T (1998) Role of cyclic GMP in olfactory transduction and adaptation. Ann N Y Acad Sci 855:199–204.

Zufall F, Leinders-Zufall T, Greer CA (2000) Amplification of odor-induced Ca(2+) transients by store-operated Ca(2+) release and its role in olfactory signal transduction. J Neurophysiol 83:501–512.